

Modes of occurrence and chemical compositions of amphiboles in eclogite from the northeastern part of the Seba eclogitic basic schists in the Sambagawa metamorphic belt, central Shikoku, Japan

Naohito Kishira*, Akira Takasu* and Md. Fazle Kabir*

Abstract

Eclogite in the northeastern part of the Seba eclogitic basic schists consists mainly of garnet, omphacite, sodic-, sodic-calcic- and calcic-amphiboles (glauco-phane, winchite, barroisite, taramite, magnesiotaramite, magnesiokatophorite, edenite and ferropargasite), epidote, and phengite, along with small amounts of albite, dolomite, quartz, rutile, titanite, biotite, tourmaline and hematite. Amphiboles in the northeastern part of the Seba eclogitic basic schists have a variety of modes of occurrence (Amp 1-4) and a wide range of chemical compositions, i.e. sodic-, sodic-calcic- and calcic-amphiboles. Amphiboles (Amp1) occurring as inclusions in the cores of porphyroblastic garnets are classified as sodic-calcic-amphiboles (taramite), and the rim of the garnets contain inclusions of sodic-calcic-amphiboles (Amp1; e.g. magnesiotaramite, magnesiokatophorite). Amphibole (Amp2; barroisite, magnesiotaramite, magnesiokatophorite) found as inclusions in the garnet rims occur as a constituent of amphibole and albite symplectite. Schistosity-forming amphiboles (Amp3) in the matrix are zoned, with resorbed barroisite-magnesiokatophorite cores, resorbed glauco-phane in the mantles, winchite-barroisite-magnesiotaramite-magnesiokatophorite rims, and edenite-ferropargasite outermost rims. Amphiboles (Amp4) as a constituent of symplectite after omphacite are zoned, with winchite-barroisite-magnesiokatophorite cores, resorbed glauco-phane in the mantles, and barroisite-magnesiokatophorite rims. The variety of modes of occurrence and the chemical compositions of the amphiboles probably reflect four metamorphic events: a precursor metamorphic event, first and second high-pressure eclogitic metamorphic events, and a third high-pressure epidote-amphibolite facies metamorphic event.

Key words: Sambagawa (Sanbagawa) metamorphic belt, northeastern Seba eclogitic basic schists, amphibole, glauco-phane, taramite

Introduction

Amphibole group minerals occur in a wide range of *P-T* conditions, and are common constituents of igneous and metamorphic rocks (Deer *et al.*, 1992). Amphiboles crystallize in a wide spectrum of metamorphic conditions, ranging from greenschist and blueschist facies, through epidote-amphibolite to the eclogite and lower granulite facies. Amphiboles in metamorphic rocks are often chemically zoned, and provide important information on metamorphic history.

The Sambagawa belt is a high-*P/T* metamorphic belt that stretches throughout SW Japan over a length of approximately 800 km, extending from the Kanto Mountains through Kii Peninsula and Shikoku to Kyushu, with maximum width of 50 km in Shikoku (Fig. 1). To the north the Sambagawa belt is bounded by the Ryoke metamorphic belt, which is characterized by high-*T/P* metamorphism and granitic intrusions. The Sambagawa and the Ryoke belt together form possibly the best-known example of paired metamorphic belts (e.g. Miyashiro, 1973). The boundary between the Ryoke and the Sambagawa belts is a major strike-slip fault, the Median Tectonic Line (MTL), which is associated with ancient left-lateral and recent right-lateral motions (Ichikawa, 1980).

The protoliths of the Sambagawa metamorphic belt are

dominated by sandstone and shale, with lesser basalt, chert, and limestone. Metamorphic grade ranges from prehnite-pumpellyite facies through the blueschist/greenschist facies to the epidote-amphibolite facies, and locally into the eclogite facies (e.g. Banno, 1964; Higashino, 1990; Enami *et al.*, 1994). In the Besshi district of central Shikoku, the Sambagawa belt is divided into four zones based on index minerals in pelitic schists (Enami, 1983; Higashino, 1990). These are the chlorite (300-360°C, 5.5-6.5 kbar), garnet (425-470°C, 7-8.5 kbar), albite-biotite (470-590°C, 8-9.5 kbar) and oligoclase-biotite (585-635°C, 9-11 kbar) zones (Fig. 1; Enami, 1983; Enami *et al.*, 1994). The mineral parageneses of the albite-biotite and oligoclase-biotite zones roughly coincide with those of the epidote-amphibolite facies, and their equilibrium *P-T* conditions have been estimated to be 8-11 kbar and 470-635°C (Enami *et al.*, 1994). Eclogite facies assemblages sporadically occur in metagabbros, metabasites, peridotites, and subordinate metapelites in the Besshi district (e.g. Banno *et al.*, 1976; Takasu, 1984; Kunugiza *et al.*, 1986; Takasu, 1989; Aoya, 2001; Ota *et al.*, 2004; Zaw Win Ko *et al.*, 2005; Kabir and Takasu, 2010a, b). Eclogites in the Besshi district occur mainly within block-like bodies of varying size and lithology (Kunugiza *et al.*, 1986; Takasu, 1989; Takasu *et al.*, 1994). The metamorphic *P-T* conditions of the eclogite-bearing bodies are distinct from those of surrounding Sambagawa schists (Takasu, 1989).

*Department of Geoscience, Graduate School of Science and Engineering, Shimane University, 1060 Nishikawatsu, Matsue 690-8504, Japan

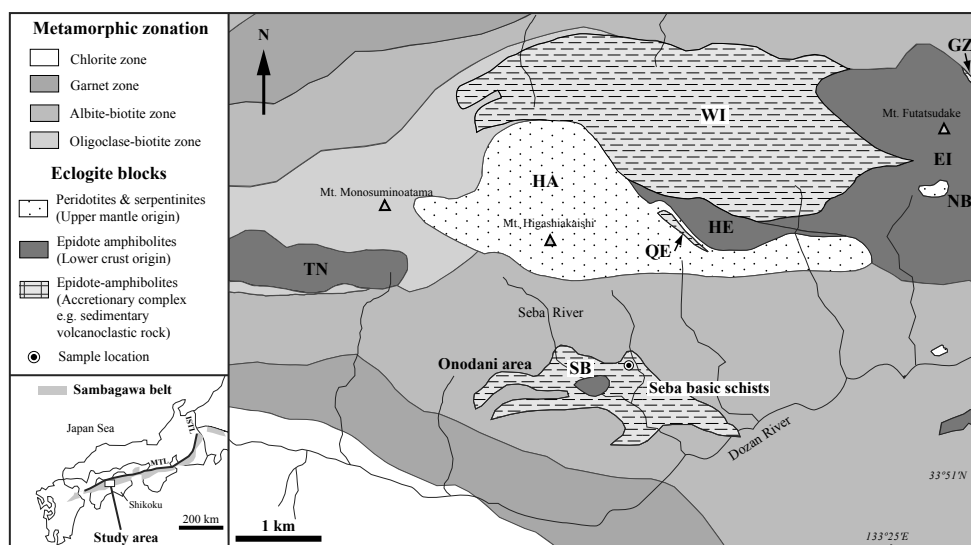


Fig. 1. Geological and metamorphic zonation map of the Sambagawa metamorphic belt in the Besshi district, central Shikoku, Japan (compiled from Takasu and Makino, 1980; Takasu, 1989; Higashino, 1990; Kugimiya and Takasu, 2002; Sakurai and Takasu, 2009; Kabir and Takasu, 2010a). SB, Seba metagabbro mass; TN, Tonaru metagabbro mass; WI, Western Iratsu mass; EI, Eastern Iratsu mass; HA, Higashi-akaishi peridotite mass; QE, Quartz eclogite mass; HE, Hornblende eclogite mass; NB, Nikubuchi peridotite mass; GZ, Gazo eclogite mass.

The Sebadani area is located in the central part of the Besshi district, within the albite-biotite zone. The Sebadani metagabbro mass and surrounding Seba basic schists, pelitic and siliceous schists occur in the area (Takasu and Makino, 1980; Takasu, 1984). Eclogitic mineral assemblages are sporadically preserved in both the Sebadani metagabbro and the Seba basic schists (Seba eclogitic basic schists) (e.g. Takasu, 1984; Naohara and Aoya, 1997; Aoya, 2001).

Aoya (2001) reported a P - T path from eclogites occurring in the Seba eclogitic basic schists. The eclogites first attained their peak pressure, then decompressed with continuously increasing temperature before reaching their peak temperature (610–640°C and 12–24 kbar). The eclogites were then retrograded at epidote-amphibolite conditions, and were subsequently emplaced into the surrounding non-eclogitic schists at the time of prograde epidote-amphibolite metamorphism (Aoya, 2001; Zaw Win Ko *et al.*, 2005). The Onodani eclogites preserved within the Seba basic schists have a complex metamorphic history, undergoing three differing metamorphic episodes during multiple burial and exhumation cycles (Kabir and Takasu, 2010a). Conditions of the first and second eclogite facies metamorphism are estimated to have been 530–590°C and 19–21 kbar and 630–680°C and 20–22 kbar, respectively. The second metamorphic event is similar to that of the Seba eclogitic basic schists (610–640°C and 12–24 kbar; Aoya, 2001). The pelitic schists intercalated within the Seba eclogitic basic schists also underwent eclogite facies metamorphism of 520–550°C and *c.* 18 kbar (Zaw Win Ko *et al.*, 2005; Kouketsu *et al.*, 2010). Owing to the complex metamorphic history of the Seba eclogitic basic schists, amphiboles within them have varying modes of occurrence and a variety of chemical compositions.

In this report we describe the diverse textures and variable chemical compositions of the amphiboles in the eclogite from the northeastern part of the Seba eclogitic basic schists. The amphibole classification follows Leake *et al.* (1997), and mineral abbreviations used in the text, tables and figures follow Whitney and Evans (2010).

Petrography of the northeastern part of the Seba eclogitic basic schists

Several eclogite samples were collected from the northeastern part of the Seba eclogitic basic schists (hereafter termed eclogite). One eclogite sample (KSB-5) was selected for detail petrography. The eclogite consists mainly of garnet, omphacite, sodic-, sodic-calcic- and calcic-amphiboles (glaucofanite, winchite, barrosite, taramite, magnesirotaramite, magnesiokatophorite, edenite and ferropargasite), epidote, and phengite (Fig. 2). Small amounts of albite, dolomite, quartz, rutile, titanite and biotite, tourmaline and hematite occur occasionally. A schistosity is defined by preferred orientation of omphacite, amphibole, epidote and phengite.

Garnets occur as euhedral to subhedral grains up to 1 mm in diameter. Some are zoned, with pale orange cores to colorless rims. The garnet cores contain inclusions of taramitic amphiboles (Fig. 3a), whereas the rims contain inclusions of omphacite (X_{Id} 0.27–0.41), sodic-calcic-amphiboles (e.g. magnesirotaramite, magnesiokatophorite), epidote (X_{Ps} 0.23–0.26), dolomite, hematite and quartz. The rims of the garnets also contain sodic-calcic-amphibole (barrosite, magnesirotaramite, magnesiokatophorite)-albite ($An < 1$) symplectite (Fig. 3b-c). Some garnets are partly replaced by chlorite.

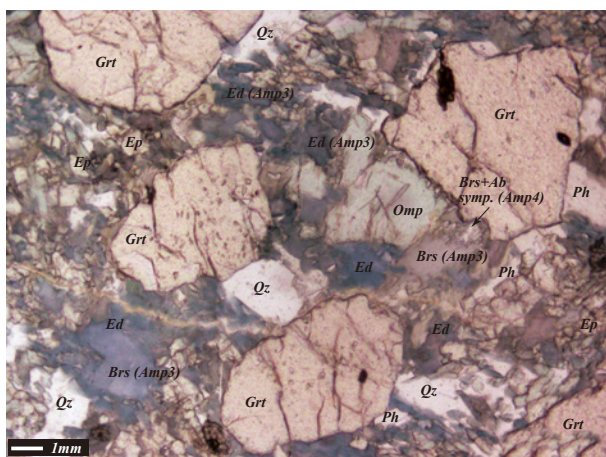


Fig. 2. Photomicrograph of eclogite from the northeastern part of the Seba eclogitic basic schists, showing eclogite facies mineral assemblages of porphyroblastic garnet and coexisting omphacite, phengite and barroisitic amphibole.

Omphacites occur as anhedral grains up to 0.5 mm across, and some are zoned from pale green cores to colorless rims (X_{Jd} 0.27-0.43, A_e 0.11-0.17). The omphacites contain inclusions of epidote (X_{Ps} 0.22-0.24), and are partly replaced by amphibole (barroisite/magnesiokatophorite) + albite ($An < 1$) symplectite.

Amphiboles have four modes of occurrence, being found as discrete inclusions in garnet cores (Amp1); as amphibole (Amp2) + albite symplectite inclusions in garnet rims; as schistosity-forming amphibole (Amp3), and as a constituent of amphibole (Amp4) + albite symplectite after omphacite (Fig. 3a-f). Amphibole (Amp1; sodic-calcic-amphibole) occurring as inclusions in the garnet cores is found as anhedral crystals up to 0.02 mm across (Fig. 3a). Amphibole (Amp2; sodic-calcic-amphibole) found as inclusions in the garnet rims occur as anhedral crystals up to 0.1 mm across. These amphiboles occur as a constituent of amphiboles and albite symplectite, and some are zoned, with cores of barroisite mantled by magnesiokatophorite/magnesiokatophorite, and barroisite rims (Fig. 3b-c). Schistosity-forming amphibole (Amp3) in the matrix occurs as anhedral to subhedral grains up to 0.5 mm across, some of which are zoned, with resorbed barroisite-magnesiokatophorite cores, resorbed glaucophane in the mantles, winchite-barroisite-magnesiokatophorite rims, and edenite-ferropargasite outermost rims (Fig. 3d-e). Amphiboles in the matrix contain inclusions of omphacite (X_{Jd} 0.37-0.40), epidote (X_{Ps} 0.21-0.27), hematite and quartz. Symplectitic amphibole (Amp4) comprises anhedral grains up to 0.1 mm across, some of which are zoned, with winchite-barroisite-magnesiokatophorite cores, resorbed glaucophane in the mantles, and barroisite-magnesiokatophorite rims (Fig. 3f).

Epidote occurs as anhedral grains up to 0.2 mm across; some are zoned, from yellowish-green cores to colorless rims. Epidote contains quartz inclusions. Two modes of occurrence of phengite were observed. Schistosity-forming phengite (Si 6.65-6.87 pfu) is found as subhedral grains up

to 1 cm across. Other phengites are randomly oriented (Si 6.34-6.56 pfu), and also reach 1 cm in width.

Chemical compositions of the amphiboles

Chemical composition and compositional zoning of the amphiboles in the northeastern part of the Seba eclogitic basic schists were investigated at Shimane University, using JEOL JXA 8800M and JXA 8530F electron microprobe analyzers. Analytical conditions used for quantitative analysis were 15 kV accelerating voltage, 20 nA specimen current, and 5 μm beam diameter. Correction procedure was carried out as described by Bence and Albee (1968). Fe^{3+} estimation for amphibole used the 13cCNK method (Leake *et al.*, 1997). Cr_2O_3 contents ($\text{Cr} < 0.01$ pfu) of the amphiboles are negligible.

Representative chemical compositions of amphiboles are listed in Table 1, and shown in Figs. 4 and 5.

Amphibole (Amp1) inclusions in the garnet cores are classified as taramite, and have relatively low Si (Si = 6.10 pfu, $\text{Na}_B = 0.68$ pfu and $X_{\text{Mg}} = 0.44$), higher Al_2O_3 (15.41 wt.%), Ti (Ti = 0.08 pfu; $\text{TiO}_2 = 0.67$ wt.%) and K (0.04 pfu) contents (Figs. 4, 5c; Table 1). Amphibole inclusions in the rims of the porphyroblastic garnets are classified as sodic-calcic-amphiboles (e.g. magnesiokatophorite, magnesiokatophorite), with compositional ranges of Si = 6.42-6.79 pfu, $\text{Na}_B = 0.81$ -0.93 pfu, $X_{\text{Mg}} = 0.56$ -0.61, Ti = 0.02-0.08 pfu and K = 0.06-0.07 pfu.

Symplectitic amphibole (Amp2) inclusions in the rims of the porphyroblastic garnets are classified as sodic-calcic-amphiboles (e.g. barroisite, magnesiokatophorite), with compositional ranges of Si = 6.16-7.29 pfu, $\text{Na}_B = 0.68$ -1.12 pfu, $X_{\text{Mg}} = 0.55$ -0.67, Ti = 0.01-0.03 pfu and K = 0.04-0.13 pfu. Amp2 is sometimes zoned, from barroisite cores to magnesiokatophorite/magnesiokatophorite mantles, decreasing in Si (7.17-6.40 pfu), Na_B (1.12-0.68 pfu), X_{Mg} (0.67-0.55) and increasing Ti (0.02-0.03 pfu) and K (0.04-0.13 pfu), whereas Si (6.40-7.05 pfu), X_{Mg} (0.55-0.65), Ti (0.03-0.02 pfu) and K (0.13-0.07 pfu) increases at the barroisite rims, and Na_B (0.68-0.97 pfu) decreases (Figs. 4, 5b-c; Table 1).

Amphiboles (Amp3) in the matrix are classified as sodic-, sodic-calcic- and calcic-amphiboles (e.g. glaucophane, winchite, barroisite, magnesiokatophorite, edenite, ferropargasite), with compositional ranges of Si = 6.20-7.82 pfu, $\text{Na}_B = 0.18$ -1.78 pfu, $X_{\text{Mg}} = 0.45$ -0.77, Ti = 0.01-0.05 pfu and K = 0-0.17 pfu. The cores of the zoned amphiboles (Amp3) are classified as barroisite with Si = 7.37 pfu, $\text{Na}_B = 1.26$ pfu, $X_{\text{Mg}} = 0.68$, Ti = 0.01 pfu and K = 0.03 pfu, mantled by glaucophane, with higher Si = 7.76-7.83 pfu, $\text{Na}_B = 1.71$ -1.73 pfu and $X_{\text{Mg}} = 0.64$ -0.66 (Figs. 4, 5a-c). The barroisite rims have lower Si = 7.22 pfu, $\text{Na}_B = 0.85$ pfu, $X_{\text{Mg}} = 0.67$, Ti = 0.01 pfu and K = 0.04 pfu. The edenite-ferropargasite outermost rims have compositions of Si = 6.45-6.76 pfu, $\text{Na}_B = 0.18$ -0.49 pfu, $X_{\text{Mg}} = 0.47$ -0.54, Ti = 0.02 pfu and K = 0.11 pfu (Figs. 4 and 5d).

Amp4 is a constituent of symplectite of amphibole

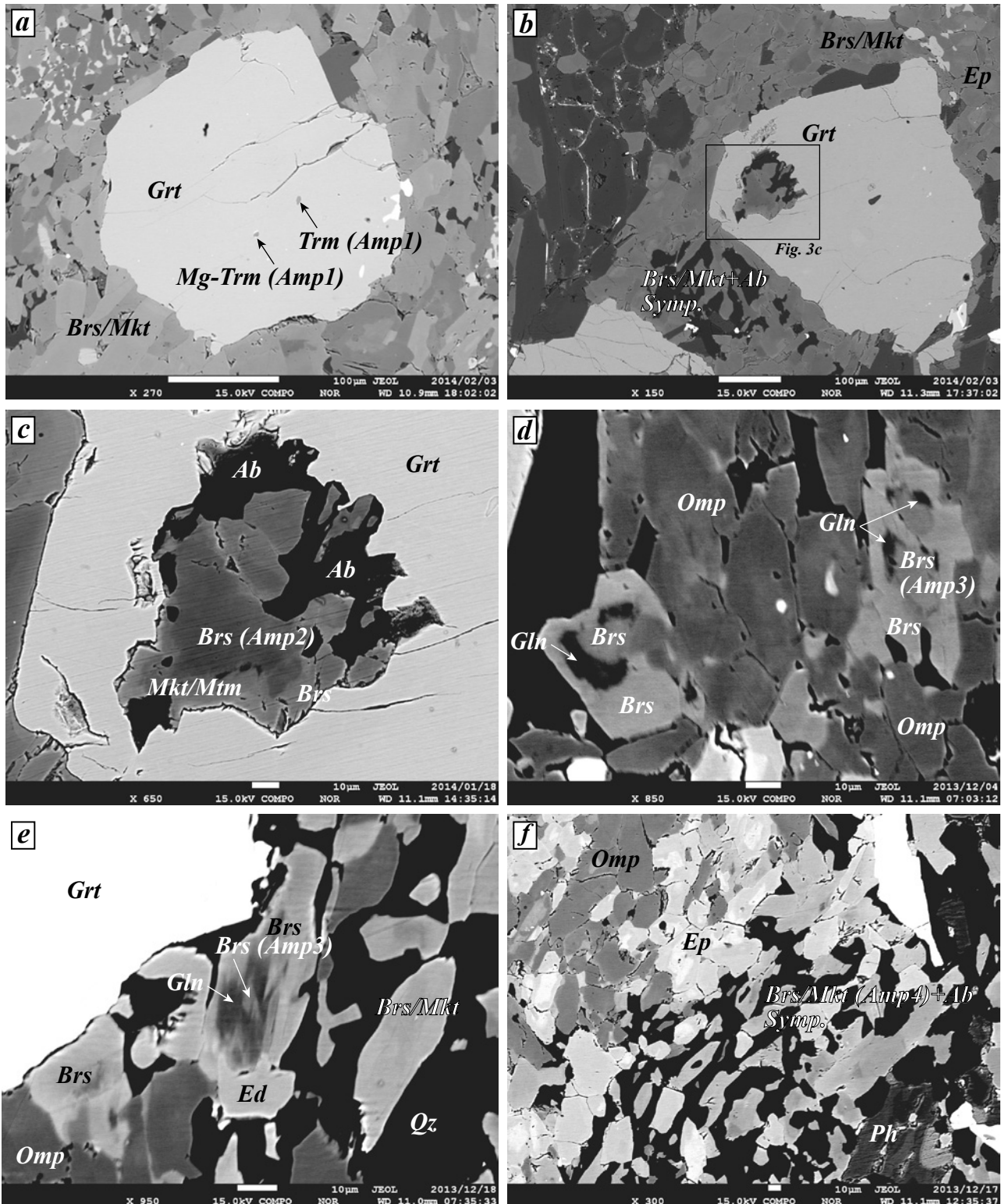


Fig. 3. Photomicrographs of eclogite from the northeastern part of the Seba eclogitic basic schists showing: (a) porphyroblastic garnet containing inclusions of taramitic amphibole (Amp1) in the core. (b-c) Rim of the porphyroblastic garnet containing inclusions of amphibole (Amp2) and albite symplectite. Barroisite/magnesiokatophorite and albite after omphacite are also shown. (d-e) Zoned amphibole (Amp3) in the matrix showing barroisite as a resorbed shape in the core, mantled by glaucophane, barroisite rims, and edenite at the outermost rim. (f) Omphacite replaced by symplectite of amphibole (Amp4; barroisite / magnesiokatophorite) and albite.

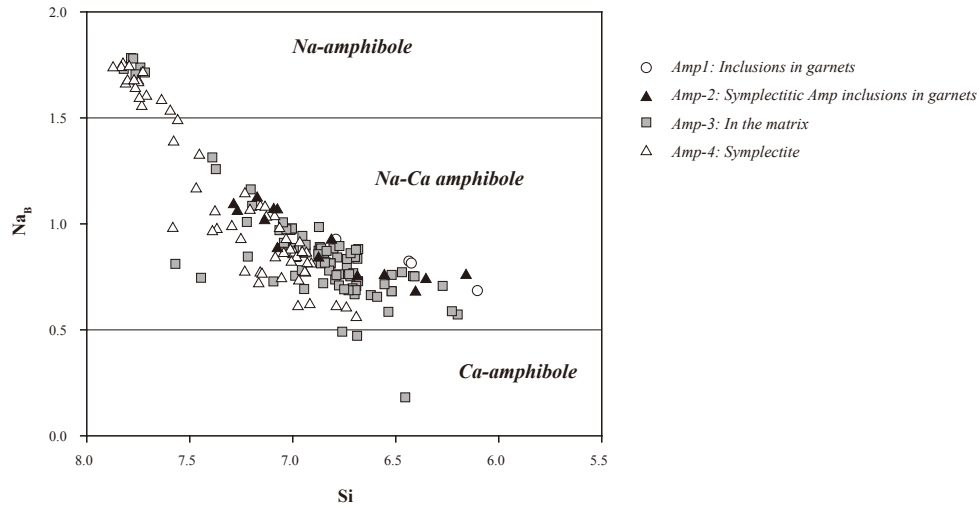


Fig. 4 Chemical compositions of amphiboles in the northeastern part of the Seba eclogitic basic schists.

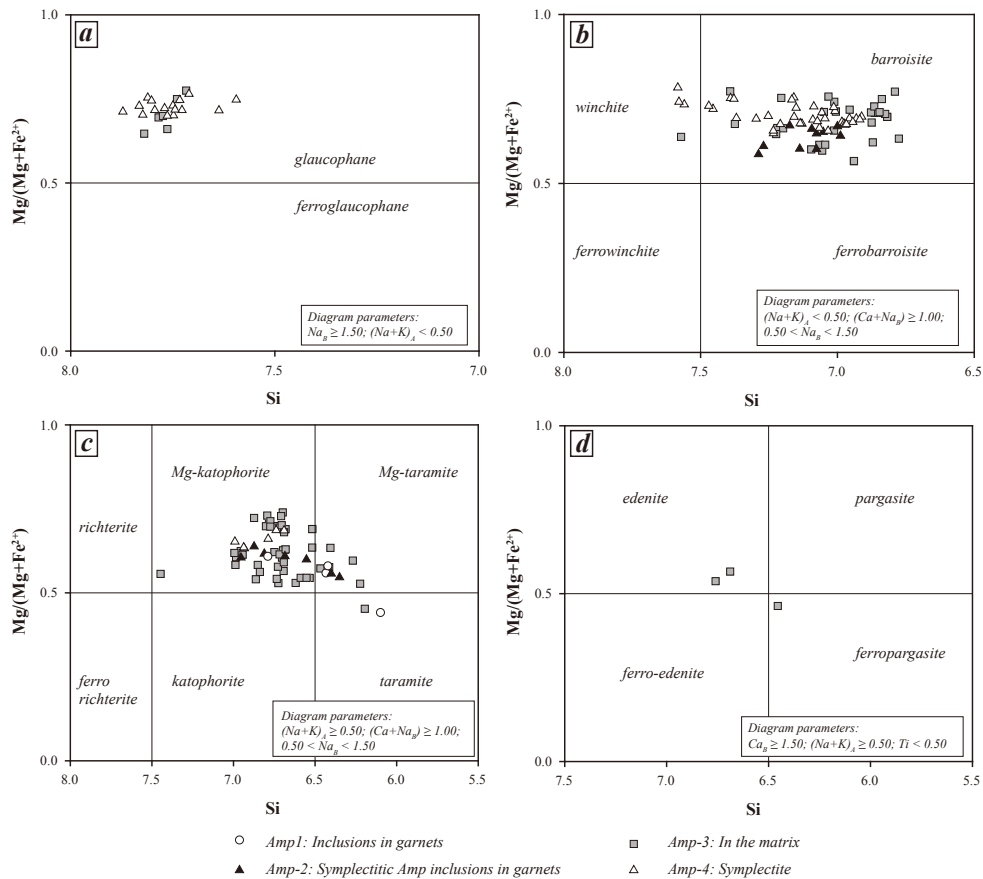


Fig. 5 Chemical compositions of sodic- (a), sodic-calcic- (b-c) and calcic (d) amphiboles from the northeastern part of the Seba eclogitic basic schists.

and albite after omphacite ($X_{\text{Id}}=0.27-0.43$), and is the analyzed grains are classified as sodic- and sodic-calcic-amphiboles. The sodic-amphiboles are glaucophane with $\text{Si}=7.60-7.87$ pfu, $\text{Na}_B=1.53-1.75$ pfu, $X_{\text{Mg}}=0.70-0.76$ and $\text{Ti}=0-0.01$ pfu. The sodic-calcic-amphiboles are represented by winchite, barroisite and magnesiokatophorite, with compositions of $\text{Si}=6.69-7.58$ pfu, $\text{Na}_B=0.56-1.49$ pfu,

$X_{\text{Mg}}=0.63-0.79$, $\text{Ti}=0.01-0.04$ pfu and $\text{K}=0.02-0.10$ pfu. Some of these are zoned, with cores consisting of winchite and barroisite with $\text{Si}=6.91-7.56$ pfu, $\text{Na}_B=0.81-1.49$ pfu, $X_{\text{Mg}}=0.68-0.74$, $\text{Ti}=0.02-0.03$ pfu and $\text{K}=0.02-0.06$ pfu; glaucophane mantles with increasing $\text{Si}=7.73$ pfu, $\text{Na}_B=1.56$ pfu, $X_{\text{Mg}}=0.74$, $\text{Ti}=0.01$ pfu and $\text{K}=0.01$ pfu; and barroisite rims with decreasing $\text{Si}=7.01-7.45$ pfu,

$Na_B = 0.71-1.32$ pfu, $X_{Mg} = 0.72-0.75$, $Ti = 0.01-0.03$ pfu and $K = 0.03-0.05$ pfu (Figs. 4 and 5a-c).

Discussion and Conclusions

Amphiboles in the eclogites from the northeastern part of the Seba eclogitic basic schists exhibit several modes of occurrence and a wide range of chemical compositions (sodic-, sodic-calcic- and calcic-amphiboles), suggesting diverse *P-T* crystallization conditions.

Taramitic amphibole (Amp1) relatively rich in Al_2O_3 (15.41 wt.%) and TiO_2 (0.67 wt.%) are thought to be relict amphibole inclusions in the cores of the porphyroblastic garnets, probably indicating relatively high-temperature metamorphic conditions such as the amphibolite facies (Kabir and Takasu, 2010c).

Symplectitic amphiboles (Amp2) together with albite are regarded as pseudomorphs after omphacite that originally occurred as inclusions in the rims of the porphyroblastic garnets. This feature suggests that this omphacite equilibrated before the growth of the porphyroblastic garnets. These earlier omphacites may be correlated with the first eclogite facies metamorphism of the Onodani eclogite (Kabir and Takasu, 2010a). Amphibole (Amp1; magnesiotaramite, magnesiokatophorite) found as inclusions in the garnets crystallized during prograde to peak metamorphism, i.e. epidote-blueschist/epidote-amphibolite to eclogite facies metamorphism.

Amp4 is a constituent of symplectite of amphibole and albite after omphacite ($X_{Id} = 0.27-0.43$), and is represented by sodic- and sodic-calcic-amphibole (winchite, barroisite, magnesiokatophorite and glaucophane). The cores of Amp4 (winchite, barroisite, magnesiokatophorite to glaucophane) probably formed during the prograde metamorphism, whereas the rims (barroisite, magnesiokatophorite) formed in epidote-amphibolite facies conditions during retrograde metamorphism (Kabir and Takasu, 2010a).

Amphibole in the matrix (Amp3) is strongly zoned, with resorbed barroisite cores, glaucophane mantles, winchite-barroisite-magnesiokatophorite-magnesiotaramite rims, and edenite-ferropargasite outermost rims. This occurrence probably corresponds to the third high-pressure metamorphic event identified by Kabir and Takasu (2010a, b), and was stable under the glaucophane schist facies to the epidote-amphibolite facies conditions prevailing at the metamorphic peak, and in lower-grade greenschist facies conditions during subsequent retrograde metamorphism.

Acknowledgements

We thank members of the Metamorphic Geology seminar of Shimane University for discussion and helpful suggestions, and B. P. Roser for critical reading and comments on the manuscript. Thanks are also due to Yasunori Kondo for his support during fieldwork. This study was partly supported by JSPS KAKENHI Grant (No. 24340123) to A.T.

References

- Aoya, M., 2001, *P-T-D* path of eclogite from the Sambagawa belt deduced from combination of petrological and microstructural analyses. *Journal of Petrology*, **42**, 1225-1248.
- Banno, S., 1964, Petrological studies of the Sanbagawa crystalline schists in the Bessi-Iino district, central Shikoku, Japan. *Journal of the Faculty of Science, Tokyo University, Section II*, **15**, 203-319.
- Banno, S., Yokohama, K., Enami, M., Iwata, O., Nakamura, K. and Kasashima, S., 1976, Petrography of the peridotite-metagabbro complex in the vicinity of Mt. Higashi-akaishi, Central Shikoku. Part I. Megascopic textures of the Iratsu and Tonaru epidote amphibolite massas. *The Science Reports of Kanazawa University*, **21**, 139-159.
- Bence, A. E. and Albee, A. L., 1968, Empirical correction factors for the electron microanalysis of silicates and oxides. *Journal of Geology*, **76**, 382-403.
- Deer, W. A., Howie, R. A. and Zussman, J., 1992, *An introduction to the rock-forming minerals*. Longman Scientific & Technical, Harlow, England.
- Enami, M., 1983, Petrology of pelitic schists in the oligoclase-biotite zone of the Sanbagawa metamorphic terrain, Japan: phase equilibria in the highest grade zone of a high-pressure intermediate type of metamorphic belt. *Journal of Metamorphic Geology*, **1**, 141-161.
- Enami, M., Wallis, S. R. and Banno, Y., 1994, Paragenesis of sodic-pyroxene-bearing quartz schists: implications for the *P-T* history of the Sanbagawa belt. *Contributions to Mineralogy and Petrology*, **116**, 182-198.
- Higashino, T., 1990, The higher grade metamorphic zonation of the Sambagawa metamorphic belt in central Shikoku, Japan. *Journal of Metamorphic Geology*, **8**, 413-423.
- Ichikawa, K., 1980, Geohistory of the Median Tectonic Line of southwest Japan. *Memoirs of the Geological Society of Japan*, **18**, 187-212.
- Kabir, M. F. and Takasu, A., 2010a, Evidence for multiple burial-partial exhumation cycles from the Onodani eclogites in the Sambagawa metamorphic belt, central Shikoku, Japan. *Journal of Metamorphic Geology*, **28**, 873-893.
- Kabir, M. F. and Takasu, A., 2010b, Glaucophanic amphibole in the Seba eclogitic basic schists, Sambagawa metamorphic belt, central Shikoku, Japan: implications for timing of juxtaposition of the eclogite body with the non-eclogite Sambagawa schists. *Earth Sciences*, **64**, 183-192.
- Kabir, M. F. and Takasu, A., 2010c, Polyphase high-pressure metamorphism of eclogites and associated pelitic schists in the Sebadani and Onodani areas, Sambagawa metamorphic belt, central Shikoku, Japan. In: *Annual Meeting, Japan Association of Mineralogical Sciences*, pp. 205, Shimane University, Japan.
- Kouketsu, Y., Enami, M. and Mizukami, T., 2010, Omphacite-bearing metapelite from the Besshi region, Sambagawa metamorphic belt, Japan: Prograde eclogite facies metamorphism recorded in metasediment. *Journal of Mineralogical and Petrological Sciences*, **105**, 9-19.
- Kugimiyama, Y. and Takasu, A., 2002, Geology of the Western Iratsu mass within the tectonic melange zone in the Sambagawa metamorphic belt, Besshi district, central Shikoku, Japan. *Journal of the Geological Society of Japan*, **108**, 644-662.
- Kunugiza, K., Takasu, A. and Banno, S., 1986, The origin and metamorphic history of the ultramafic and metagabbro bodies in the Sanbagawa Metamorphic Belt. *Geological Society of America Memoir*, **164**, 375-386.
- Leake, B. E., Woolley, A. R., Arps, C. E. R., Birch, W. D., Gilbert, M. C., Grice, J. D., Hawthorne, F. C., Kato, A., Kisch, H. J., Krivovichev, V. G., Linthout, K., Laird, J., Mandarino, J. A., Maresch, W. V., Nickel, E. H., Rock, N. M. S., Schumacher, J. C., Smith, D. C., Stephenson, N. C. N., Ungaretti, L., Whittaker, E. J. W. and Youzhi, G., 1997, Nomenclature of amphiboles: report of the subcommittee on amphiboles of the International Mineralogical Association, Commission on New Minerals and Mineral Names. *The Canadian Mineralogist*, **35**, 219-246.
- Miyashiro, A., 1973, *Metamorphism and metamorphic belts*. George Allen and Unwin, London, England.
- Naohara, R. and Aoya, M., 1997, Prograde eclogites from Sambagawa basic schists in the Sebadani area, central Shikoku, Japan. *Memoirs of the Faculty of Science and Engineering, Shimane University. Series A*, 63-73.

- Ota, T., Terabayashi, M. and Katayama, I., 2004, Thermobaric structure and metamorphic evolution of the Iratsu eclogite body in the Sanbagawa belt, central Shikoku, Japan. *Lithos*, **73**, 95-126.
- Sakurai, T. and Takasu, A., 2009, Geology and metamorphism of the Gazo mass (eclogite-bearing tectonic block) in the Sanbagawa metamorphic belt, Besshi district, central Shikoku, Japan. *Journal of the Geological Society of Japan*, **115**, 101-121.
- Takasu, A., 1984, Prograde and retrograde eclogites in the Sanbagawa metamorphic belt, Besshi district, Japan. *Journal of Petrology*, **25**, 619-643.
- Takasu, A., 1989, *P-T* histories of peridotite and amphibolite tectonic blocks in the Sanbagawa metamorphic belt, Japan. In: *Evolution of Metamorphic Belts* (eds Daly, J. S., Cliff, R. A. & Yardley, B. W. D.), pp. 533-538, Blackwell Scientific Publications, Oxford, Geological Society, London, Special Publications.
- Takasu, A. and Makino, K., 1980, Stratigraphy and geologic structure of the Sanbagawa metamorphic belt in the Besshi district, Shikoku, Japan (Reexamination of the recumbent fold structures). *Earth Science (Chikyū Kagaku)*, **34**, 16-26 (in Japanese with English abstract).
- Takasu, A., Wallis, S. R., Banno, S. and Dallmeyer, R. D., 1994, Evolution of the Sanbagawa metamorphic belt, Japan. *Lithos*, **33**, 119-133.
- Whitney, D. L. and Evans, B. W., 2010, Abbreviations for names of rock-forming minerals. *American Mineralogist*, **95**, 185-187.
- Zaw Win Ko, Enami, M. and Aoya, M., 2005, Chloritoid and barroisite-bearing pelitic schists from the eclogite unit in the Besshi district, Sanbagawa metamorphic belt. *Lithos*, **81**, 79-100.

(Received: Nov. 12, 2013, Accepted: Dec. 5, 2013)

(要 旨)

岸良尚人・高須 晃・Kabir Md. Fazle, 2013 四国中央部三波川変成帯瀬場エクロジヤイト質塩基性片岩体北東部に分布するエクロジヤイト中の角閃石の産状と化学組成. 島根大学地球資源環境学術研究報告, **32**, 33-42.

四国中央部別子地域に三波川変成帯瀬場エクロジヤイト質塩基性片岩体の北東縁部のエクロジヤイトの構成鉱物は、ざくろ石、オンファス輝石、角閃石（藍閃石、ウインチ閃石、バロア閃石、タラマ閃石、苦土タラマ閃石、苦土カトホル閃石、エデン閃石、鉄パーガス閃石）、緑れん石、フェンジャイト、曹長石、石英、方解石、ドロマイト、黒雲母、電気石、チタン石、ルチル、鉄鉱類である。エクロジヤイト中の角閃石は4つの産状に分類される。ざくろ石のコアの包有物の角閃石（Amp1）はタラマ閃石で、ざくろ石の成長前に高温の変成作用を経験したことが示唆される。ざくろ石のリムに包有される角閃石（Amp2）と曹長石からなるシンプレクタイトは、ざくろ石の形成以前にオンファス輝石が存在し、それが分解したことによって形成したと考えられる。これより、ざくろ石の形成以前にエクロジヤイト相条件にあったことが推測できる。基質の角閃石（Amp3）は、融食したバロア閃石のコア、さらに藍閃石のマントル、ウインチ閃石／バロア閃石／苦土カトホル閃石／苦土タラマ閃石のリム、そしてエデン閃石／鉄パーガス閃石の最外縁部のリムの累帯構造を示す。基質にある角閃石（Amp4）と曹長石からなるシンプレクタイトを構成する角閃石は累帯構造を示し、ウインチ閃石／バロア閃石／苦土カトホル閃石のコア、藍閃石のマントル、バロア閃石／苦土カトホル閃石のリムからなる。このような多様な角閃石の産状と化学組成は、4つの変成イベントに対応する。すなわち、先駆的変成イベント、第一および第二エクロジヤイト相変成イベント、高圧緑れん石角閃岩相イベントである。

Table 1. Representative chemical compositions of amphiboles from the northeastern part of the Seba eclogitic basic schists.

Sample	KSB-5																			
Analysis	28	34	46	50	52	59	60	61	74	75	76	90	271	272	90	277	283	284	287	
	Amp3	Amp3	Amp3	Amp3	Amp3	Amp3	Amp3	Amp3	Amp3	Amp3	Amp3	Amp3	Amp3	Amp3	Amp3	Amp3	Amp3	Amp3	Amp3	Amp3
	Mkt	Mkt	Mtm	Mkt	Mtm	Mtm	Mkt	Mtm	Mkt	Mkt	Mkt	Mkt	Mkt	Mkt	Mkt	Mkt	Mkt	Mkt	Mkt	Mkt
SiO ₂	46.00	45.88	43.68	46.30	43.90	43.70	44.34	42.36	46.15	46.50	45.56	44.44	47.81	47.05	44.44	47.44	47.47	48.46	46.36	
TiO ₂	0.20	0.31	0.18	0.34	0.22	0.27	0.31	0.37	0.35	0.31	0.25	0.27	0.29	0.37	0.27	0.29	0.29	0.27	0.34	
Al ₂ O ₃	12.06	12.28	14.49	12.14	14.14	13.61	12.97	14.97	11.13	11.09	11.42	12.46	11.52	11.39	12.46	10.88	11.32	10.83	11.54	
FeO*	16.88	16.77	17.08	16.78	16.82	17.10	16.32	16.77	14.96	14.62	15.18	15.39	15.26	15.41	15.39	14.10	14.70	14.42	15.44	
MnO	0.28	0.27	0.27	0.32	0.24	0.26	0.21	0.23	0.27	0.18	0.22	0.19	0.20	0.22	0.19	0.18	0.22	0.24	0.26	
MgO	9.84	9.47	8.76	9.82	8.86	9.51	9.87	8.91	11.22	11.34	11.07	10.89	11.29	11.49	10.89	12.25	11.77	12.00	11.19	
CaO	7.48	7.31	7.92	7.46	7.78	7.94	7.88	8.15	7.69	7.41	8.08	8.38	7.31	8.15	8.38	8.23	8.44	7.41	8.36	
Na ₂ O	4.65	4.72	4.67	4.60	4.81	4.48	4.56	4.52	4.50	4.58	4.22	4.16	4.79	4.35	4.16	4.20	4.15	4.83	4.14	
K ₂ O	0.41	0.42	0.55	0.45	0.55	0.55	0.53	0.70	0.40	0.35	0.47	0.59	0.38	0.50	0.59	0.50	0.47	0.33	0.53	
Total	97.80	97.43	97.60	98.21	97.32	97.42	96.99	96.98	96.67	96.38	96.47	96.77	98.85	98.93	96.77	98.07	98.83	98.79	98.16	
<i>Cations on the basis of 23 oxygens</i>																				
Si	6.69	6.70	6.42	6.70	6.47	6.41	6.52	6.27	6.74	6.78	6.68	6.52	6.80	6.72	6.52	6.79	6.78	6.88	6.69	
Ti	0.02	0.03	0.02	0.04	0.02	0.03	0.03	0.04	0.04	0.03	0.03	0.03	0.03	0.04	0.03	0.03	0.03	0.03	0.04	
Al	2.07	2.11	2.51	2.07	2.46	2.35	2.25	2.61	1.91	1.91	1.97	2.15	1.93	1.92	2.15	1.84	1.91	1.81	1.96	
Fe ²⁺	0.79	0.70	0.69	0.77	0.62	0.90	0.76	0.74	0.77	0.78	0.77	0.82	0.78	0.76	0.82	0.72	0.66	0.74	0.73	
Fe ³⁺	1.26	1.35	1.41	1.26	1.45	1.20	1.24	1.33	1.05	1.01	1.09	1.07	1.04	1.08	1.07	0.97	1.09	0.98	1.13	
Mn	0.03	0.03	0.03	0.04	0.03	0.03	0.03	0.03	0.03	0.02	0.03	0.02	0.03	0.02	0.03	0.02	0.03	0.03	0.03	
Mg	2.13	2.06	1.92	2.12	1.95	2.08	2.16	1.97	2.44	2.47	2.42	2.38	2.39	2.45	2.38	2.61	2.50	2.54	2.41	
Ca	1.17	1.14	1.25	1.16	1.23	1.25	1.24	1.29	1.20	1.16	1.27	1.32	1.11	1.25	1.32	1.26	1.29	1.13	1.29	
Na	1.31	1.34	1.33	1.29	1.38	1.28	1.30	1.30	1.27	1.29	1.20	1.18	1.32	1.21	1.18	1.17	1.15	1.33	1.16	
K	0.08	0.08	0.10	0.08	0.10	0.10	0.10	0.13	0.08	0.06	0.09	0.11	0.07	0.09	0.11	0.09	0.09	0.06	0.10	
Total	15.55	15.54	15.68	15.53	15.71	15.63	15.63	15.71	15.53	15.51	15.55	15.60	15.51	15.55	15.60	15.50	15.53	15.53	15.55	
*Total Fe as FeO																				
Sample	KSB-5																			
Analysis	288	292	107	107	111	112	117	120	128	133	134	136	137	60	93	98	100	2	6	
	Amp3	Amp3	Amp3	Amp3	Amp3	Amp3	Amp3	Amp3	Amp3	Amp3	Amp3	Amp3	Amp3	Amp3	Amp3	Amp3	Amp3	Amp3	Amp3	Amp3
	Mkt	Mkt	Mkt	Mkt	Mkt	Mtm	Mkt	Mkt	Mkt	Mkt	Mkt	Mkt	Mkt	Mkt	Mkt	Mkt	Mkt	Mkt	Mtm	Mkt
SiO ₂	46.96	46.85	43.96	44.94	46.26	40.55	47.10	43.69	45.47	46.22	44.61	47.53	45.34	43.91	46.86	45.12	47.74	41.67	46.57	
TiO ₂	0.29	0.29	0.28	0.18	0.18	0.17	0.30	0.44	0.24	0.27	0.22	0.29	0.42	0.37	0.29	0.33	0.36	0.26	0.33	
Al ₂ O ₃	11.54	11.10	12.01	11.56	11.69	15.55	10.31	12.03	12.41	10.82	11.56	10.30	11.54	12.66	9.74	10.19	11.21	13.98	11.14	
FeO*	15.18	14.95	17.92	18.20	16.34	18.40	15.56	17.97	17.31	16.31	17.04	15.55	16.54	16.53	15.55	16.82	14.35	19.22	17.61	
MnO	0.21	0.19	0.23	0.30	0.33	0.28	0.24	0.25	0.20	0.31	0.22	0.26	0.27	0.25	0.25	0.18	0.23	0.18	0.23	
MgO	11.63	12.02	8.58	8.49	9.03	6.96	10.00	9.00	8.58	9.75	9.22	10.52	9.58	9.03	10.68	10.23	10.26	8.33	9.14	
CaO	8.06	8.50	8.28	7.72	7.33	8.72	7.27	8.83	7.34	8.06	8.17	7.77	8.26	8.36	8.24	8.16	7.09	8.82	7.52	
Na ₂ O	4.58	4.00	4.12	4.48	5.04	4.35	4.47	4.08	4.71	4.20	4.19	4.24	4.18	4.51	4.10	4.02	4.65	4.55	4.47	
K ₂ O	0.46	0.48	0.70	0.50	0.37	0.89	0.34	0.62	0.40	0.46	0.57	0.43	0.49	0.56	0.56	0.64	0.36	0.73	0.39	
Total	98.91	98.38	96.08	96.37	96.57	95.87	95.59	96.91	96.66	96.40	95.80	96.89	96.62	96.18	96.27	95.69	96.25	97.74	97.40	
<i>Cations on the basis of 23 oxygens</i>																				
Si	6.71	6.71	6.62	6.73	6.86	6.20	6.99	6.54	6.74	6.85	6.70	6.96	6.73	6.59	6.95	6.75	6.99	6.23	6.84	
Ti	0.03	0.03	0.03	0.02	0.02	0.02	0.03	0.05	0.03	0.03	0.03	0.03	0.05	0.04	0.03	0.04	0.04	0.03	0.04	
Al	1.94	1.87	2.13	2.04	2.04	2.80	1.80	2.12	2.17	1.89	2.05	1.78	2.02	2.24	1.70	1.80	1.94	2.46	1.93	
Fe ²⁺	0.76	0.83	0.55	0.59	0.33	0.44	0.49	0.57	0.54	0.48	0.55	0.52	0.51	0.39	0.44	0.71	0.38	0.74	0.61	
Fe ³⁺	1.06	0.96	1.71	1.68	1.70	1.91	1.44	1.68	1.60	1.54	1.59	1.38	1.55	1.69	1.49	1.39	1.38	1.66	1.56	
Mn	0.03	0.02	0.03	0.04	0.04	0.04	0.03	0.03	0.02	0.04	0.03	0.03	0.03	0.03	0.03	0.02	0.03	0.02	0.03	
Mg	2.48	2.57	1.93	1.90	2.00	1.59	2.21	2.01	1.90	2.16	2.06	2.30	2.12	2.02	2.36	2.28	2.24	1.86	2.00	
Ca	1.23	1.30	1.34	1.24	1.17	1.43	1.15	1.42	1.17	1.28	1.31	1.22	1.31	1.34	1.31	1.31	1.11	1.41	1.18	
Na	1.27	1.11	1.20	1.30	1.45	1.29	1.29	1.18	1.35	1.21	1.22	1.20	1.20	1.31	1.18	1.17	1.32	1.32	1.27	
K	0.08	0.09	0.13	0.10	0.07	0.17	0.07	0.12	0.08	0.09	0.11	0.08	0.09	0.11	0.11	0.12	0.07	0.14	0.07	
Total	15.58	15.49	15.67	15.64	15.68	15.89	15.50	15.72	15.60	15.57	15.65	15.50	15.61	15.76	15.60	15.59	15.50	15.87	15.53	
*Total Fe as FeO																				
Sample	KSB-5																			
Analysis	36	37	38	39	23	36	153	156	31	32	35	138	139	51	87	89	87	89	289	
	Amp3	Amp3	Amp3	Amp3	Amp3	Amp3	Amp3	Amp3	Amp3	Amp3	Amp3	Amp3	Amp3	Amp3	Amp3	Amp3	Amp3	Amp3	Amp3	Amp3
	Mkt	Mkt	Mkt	Mkt	Brs	Brs	Brs	Brs	Brs	Brs	Brs	Brs	Brs	Brs	Brs	Brs	Brs	Brs	Brs	Brs
SiO ₂	46.07	46.20	45.84	44.33	47.10	48.31	52.04	49.94	50.22	48.69	46.71	47.41	48.12	47.69	49.00	46.99	49.00	46.99	48.27	
TiO ₂	0.25	0.19	0.20	0.25	0.25	0.15	0.11	0.11	0.18	0.26	0.20	0.20	0.13	0.29	0.24	0.33	0.24	0.33	0.22	
Al ₂ O ₃	12.34	12.39	12.48	13.19	11.08	8.64	9.49	7.52	9.72	10.51	11.74	10.43	10.64	11.26	10.63	10.98	10.63	10.98	11.09	
FeO*	16.60	16.97	17.13	17.61	16.76	16.70	14.80	16.38	15.09	15.50	16.75	15.08	15.33	15.64	14.16	14.87	14.16	14.87	14.94	
MnO	0.24	0.29	0.27	0.28	0.17	0.20	0.22	0.28	0.23	0.22	0.27	0.21	0.27	0.27	0.20	0.20	0.20	0.20	0.17	
MgO	9.54	9.72	9.22	8.65	9.81	10.58	10.62	11.48	10.78	10.61	9.86	9.88	9.88	10.53	11.52	11.29	11.52	11.29	11.55	
CaO	7.28	7.22	7.17	8.11	7.10	8.08	4.88	7.46	5.96	6.67	7.11	6.99	6.54	6.57	6.67	7.64	6.67	7.64	7.33	
Na ₂ O	4.62	4.83	4.93	4.47	4.46	4.08	5.25	4.17	5.07	4.										

Table 1. (continued)

Sample	KSB-5																		
Analysis	290	297	298	299	300	106	94	99	5	143	269	33	34	153	154	155	156	157	158
	Amp3	Amp3	Amp3	Amp3	Amp3	Amp3	Amp3	Amp3	Amp3	Amp3	Amp3	Amp3	Amp3	Amp3	Amp3	Amp3	Amp3	Amp3	Amp3
	Brs	Brs	Brs	Brs	Brs	Brs	Brs	Brs	Brs	Wnc	Gln	Gln	Gln	Brs	Gln	Gln	Brs	Fe-Prg	Ed
	Core													→		→		Rim	
SiO ₂	48.30	53.56	50.07	48.16	46.79	47.00	50.02	48.36	47.51	51.33	56.60	56.29	55.91	52.04	55.73	55.73	49.94	42.71	45.38
TiO ₂	0.29	0.10	0.19	0.25	0.29	0.25	0.20	0.33	0.19	0.11	0.00	0.01	0.00	0.11	0.02	0.01	0.11	0.15	0.16
Al ₂ O ₃	11.25	9.69	11.00	11.04	10.27	10.81	10.16	11.24	10.59	6.61	9.69	9.72	9.70	9.49	9.67	9.24	7.52	12.14	9.91
FeO*	14.09	12.80	13.79	14.64	13.72	17.08	13.88	14.23	18.15	13.73	12.15	13.10	13.05	14.80	13.55	13.62	16.38	19.00	18.50
MnO	0.24	0.16	0.20	0.18	0.22	0.21	0.16	0.18	0.15	0.22	0.10	0.16	0.16	0.22	0.17	0.12	0.28	0.30	0.27
MgO	11.75	12.26	11.71	11.87	12.59	9.17	10.81	10.26	9.11	11.58	11.43	10.15	10.11	10.62	9.86	9.73	11.48	8.54	9.64
CaO	7.50	4.64	6.58	7.77	7.99	7.17	6.40	6.98	7.02	7.52	1.95	1.47	1.47	4.88	1.97	1.79	7.46	11.23	9.45
Na ₂ O	4.59	5.50	4.96	4.52	4.11	4.48	4.79	4.66	4.54	3.53	6.50	6.78	6.73	5.25	6.57	6.66	4.17	3.22	3.79
K ₂ O	0.41	0.18	0.36	0.37	0.47	0.35	0.25	0.34	0.37	0.21	0.10	0.03	0.03	0.16	0.04	0.03	0.24	0.56	0.56
Total	98.42	98.89	98.86	98.80	96.45	96.52	96.67	96.58	97.63	94.84	98.52	97.71	97.16	97.57	97.58	96.92	97.58	97.85	97.66
<i>Cations on the basis of 23 oxygens</i>																			
Si	6.88	7.39	7.05	6.84	6.79	6.94	7.22	7.04	6.94	7.57	7.72	7.79	7.77	7.37	7.76	7.82	7.22	6.45	6.76
Ti	0.03	0.01	0.02	0.03	0.03	0.03	0.02	0.04	0.02	0.01	0.00	0.00	0.00	0.01	0.00	0.00	0.01	0.02	0.02
Al	1.89	1.58	1.83	1.85	1.76	1.88	1.73	1.93	1.82	1.15	1.56	1.58	1.59	1.58	1.59	1.53	1.28	2.16	1.74
Fe ²⁺	0.67	0.74	0.63	0.73	0.87	0.57	0.41	0.35	0.71	0.26	0.70	0.58	0.60	0.69	0.51	0.47	0.74	0.20	0.49
Fe ³⁺	1.01	0.74	0.99	1.02	0.80	1.54	1.27	1.39	1.51	1.44	0.69	0.93	0.92	1.07	1.07	1.13	1.24	2.20	1.82
Mn	0.03	0.02	0.02	0.02	0.03	0.03	0.02	0.02	0.02	0.03	0.01	0.02	0.02	0.03	0.02	0.01	0.03	0.04	0.03
Mg	2.49	2.52	2.46	2.52	2.72	2.02	2.33	2.23	1.98	2.55	2.32	2.09	2.10	2.24	2.05	2.03	2.47	1.92	2.14
Ca	1.14	0.69	0.99	1.18	1.24	1.13	0.99	1.09	1.10	1.19	0.29	0.22	0.22	0.74	0.29	0.27	1.15	1.82	1.51
Na	1.27	1.47	1.35	1.25	1.16	1.28	1.34	1.32	1.28	1.01	1.72	1.82	1.81	1.44	1.78	1.81	1.17	0.94	1.09
K	0.07	0.03	0.06	0.07	0.09	0.07	0.05	0.06	0.07	0.04	0.02	0.00	0.00	0.03	0.01	0.01	0.04	0.11	0.11
Total	15.48	15.19	15.40	15.51	15.49	15.49	15.38	15.47	15.45	15.24	15.03	15.03	15.03	15.20	15.07	15.08	15.35	15.86	15.71

*Total Fe as FeO

Sample	KSB-5																		
Analysis	6	11	45	50	53	15	16	13	3	4	5	7	8	9	10	12	13	14	15
	Amp4	Amp4	Amp4	Amp4	Amp4	Amp4	Amp4	Amp4	Amp4	Amp4	Amp4	Amp4	Amp4	Amp4	Amp4	Amp4	Amp4	Amp4	Amp4
	Mkt	Mkt	Mkt	Mkt	Mkt	Mkt	Brs	Brs	Brs	Brs	Brs	Brs	Brs	Brs	Brs	Brs	Brs	Brs	Brs
SiO ₂	47.36	47.54	48.06	45.86	46.03	45.99	48.32	49.45	50.44	47.63	47.63	49.61	51.20	48.41	48.21	50.14	48.39	48.98	49.27
TiO ₂	0.20	0.22	0.20	0.28	0.33	0.31	0.19	0.25	0.20	0.27	0.25	0.17	0.12	0.22	0.24	0.23	0.31	0.22	0.25
Al ₂ O ₃	9.23	8.76	10.56	10.10	9.93	9.84	9.37	10.55	10.63	7.30	8.22	6.88	7.55	9.12	9.01	10.17	10.40	9.65	8.90
FeO*	17.58	17.64	14.62	16.02	15.59	15.93	15.81	14.37	14.46	17.18	17.01	16.35	14.91	16.31	16.82	14.24	14.90	14.56	14.60
MnO	0.24	0.28	0.18	0.19	0.17	0.19	0.25	0.17	0.19	0.28	0.25	0.29	0.23	0.28	0.25	0.15	0.16	0.17	0.17
MgO	10.38	10.75	10.93	11.73	11.76	11.23	11.38	11.02	10.25	11.88	11.32	11.66	11.71	10.62	10.58	11.22	11.35	11.52	12.12
CaO	7.25	7.88	7.30	9.22	8.90	8.79	7.49	6.29	5.58	8.86	8.09	7.86	6.65	6.53	6.87	6.00	7.37	7.37	7.53
Na ₂ O	4.67	4.32	4.64	3.73	3.92	3.72	4.42	4.82	5.01	3.52	3.85	4.01	4.22	4.67	4.49	4.98	4.37	4.35	3.96
K ₂ O	0.30	0.37	0.32	0.46	0.43	0.51	0.30	0.25	0.19	0.38	0.34	0.27	0.18	0.27	0.29	0.21	0.28	0.25	0.26
Total	97.21	97.76	96.81	97.58	97.06	96.51	97.53	97.17	96.94	97.30	96.96	97.10	96.77	96.44	96.76	97.34	97.53	97.07	97.06
<i>Cations on the basis of 23 oxygens</i>																			
Si	6.93	6.94	6.99	6.69	6.74	6.79	6.98	7.09	7.23	6.97	6.97	7.23	7.37	7.06	7.03	7.16	6.95	7.07	7.09
Ti	0.02	0.02	0.02	0.03	0.04	0.03	0.02	0.03	0.02	0.03	0.03	0.02	0.01	0.02	0.03	0.02	0.03	0.02	0.03
Al	1.59	1.51	1.81	1.74	1.71	1.71	1.60	1.78	1.80	1.26	1.42	1.18	1.28	1.57	1.55	1.71	1.76	1.64	1.51
Fe ²⁺	0.84	0.81	0.51	0.78	0.73	0.70	0.78	0.66	0.55	0.88	0.89	0.67	0.69	0.83	0.85	0.67	0.72	0.62	0.79
Fe ³⁺	1.32	1.34	1.26	1.17	1.17	1.27	1.13	1.06	1.18	1.23	1.19	1.32	1.10	1.16	1.20	1.03	1.07	1.14	0.96
Mn	0.03	0.03	0.02	0.02	0.02	0.02	0.03	0.02	0.02	0.03	0.03	0.04	0.03	0.03	0.03	0.02	0.02	0.02	0.02
Mg	2.27	2.34	2.32	2.55	2.57	2.47	2.45	2.35	2.19	2.59	2.47	2.54	2.51	2.31	2.30	2.39	2.43	2.48	2.60
Ca	1.14	1.23	1.14	1.44	1.40	1.39	1.16	0.97	0.86	1.39	1.27	1.23	1.03	1.02	1.07	0.92	1.13	1.14	1.16
Na	1.32	1.22	1.31	1.06	1.11	1.06	1.24	1.34	1.39	1.00	1.09	1.13	1.18	1.32	1.27	1.38	1.22	1.22	1.10
K	0.06	0.07	0.06	0.09	0.08	0.10	0.06	0.05	0.04	0.07	0.06	0.05	0.03	0.05	0.05	0.04	0.05	0.05	0.05
Total	15.52	15.51	15.49	15.57	15.59	15.54	15.45	15.35	15.28	15.45	15.42	15.41	15.23	15.37	15.38	15.34	15.38	15.40	15.31

*Total Fe as FeO

Sample	KSB-5																		
Analysis	16	18	19	20	21	22	23	24	25	26	27	29	40	41	42	43	44	46	47
	Amp4	Amp4	Amp4	Amp4	Amp4	Amp4	Amp4	Amp4	Amp4	Amp4	Amp4	Amp4	Amp4	Amp4	Amp4	Amp4	Amp4	Amp4	Amp4
	Win	Brs	Brs	Brs	Brs	Brs	Brs	Brs	Brs	Brs	Brs	Brs	Brs	Brs	Brs	Brs	Brs	Win	Brs
SiO ₂	53.83	51.81	48.50	48.63	52.80	49.70	49.93	47.90	48.00	50.16	49.92	49.97	51.57	51.01	52.76	48.87	47.84	53.36	50.78
TiO ₂	0.12	0.16	0.25	0.30	0.12	0.23	0.21	0.26	0.28	0.17	0.19	0.19	0.16	0.16	0.09	0.16	0.15	0.05	0.16
Al ₂ O ₃	9.55	6.89	8.91	8.96	9.16	10.44	10.84	9.87	10.04	7.45	7.41	7.95	7.49	8.39	8.17	9.22	9.97	5.79	8.95
FeO*	12.83	13.76	15.15	15.16	13.32	14.21	13.92	15.64	15.08	14.65	14.30	14.66	13.75	14.48	13.31	14.25	14.96	12.63	13.57
MnO	0.12	0.15	0.18	0.17	0.15	0.19	0.18	0.14	0.17	0.14	0.16	0.14	0.17	0.18	0.15	0.18	0.14	0.24	0.22
MgO	11.10	13.05	11.99	11.99	11.47	10.98	10.93	11.52	11.55	13.15	13.15	12.70	12.55	12.17	12.14	12.15	11.56	13.74	11.72
CaO	3.41	6.78	7.63	7.27	4.47	6.30	6.01	7.69	7.68	8.06	8.34	8.07	6.15	7.05	5.50	8.14	7.90	6.70	6.57
Na ₂ O	5.71	4.30	4.23	4.37	5.54	4.85	5.08	4.25	4.32	3.73	3.49	3.81	4.59	4.54	4.92	3.78	4.28	3.95	4.57
K ₂ O	0.12	0.16	0.27	0.28	0.14	0.25	0.23	0.31	0.33	0.27	0.29	0.28	0.14	0.19	0.14	0.27	0.29	0.10	0.21
Total	96.79	97.06	97.11	97.14	97.17	97.15	97.33	97.58	97.45	97.78	97.25	97.77	96.57	98.17	97.18	97.02	97.09	96.56	96.75
<i>Cations on the basis of 23 oxygens</i>																			
Si	7.56	7.39	7.01	7.01	7.45	7.13	7.14	6.91	6.93	7.16	7.17	7.15	7.38	7.25	7.47	7.06	6.94	7.58	7.30
Ti	0.01	0.02	0.03	0.03	0.01	0.03	0.02	0.03	0.03	0.02	0.02	0.02	0.02	0.02	0.01	0.02	0.02	0.01	0.02
Al	1.58	1.16	1.52	1.52	1.52	1.76	1.83	1.68	1.71	1.25	1.25	1.34	1.26</						

